Insights Imaging (2013) 4:257–272
DOI 10.1007/s13244-013-0240-1

PICTORIAL REVIEW

MRI characteristics of cysts and "cyst-like" lesions in and around the knee: what the radiologist needs to know

Evangelos Perdikakis · Vasilios Skiadas

Received: 7 November 2012 / Revised: 14 February 2013 / Accepted: 19 February 2013 / Published online: 12 March 2013

Abstract
Objectives and Methods A variety of benign cystic or "cyst-like" lesions may be encountered during a routine magnetic resonance imaging (MRI) of the knee. These lesions comprise a diverse group of entities from benign cysts to complications of underlying diseases. In addition, normal anatomic bursae and recesses may be misdiagnosed as an intra-articular cystic lesion when they are distended. However, the majority of the aforementioned lesions have characteristic MR appearances that allow a confident diagnosis, thus obviating the need for additional imaging or interventional procedures.
Results This article includes a comprehensive pictorial essay of the characteristic MRI features of common and uncommon benign cysts and "cyst-like" lesions in and around the knee joint.
Discussion For accurate assessment of the "cystic structure", a radiologist should be able to identify typical MRI patterns that contribute in establishing the correct diagnosis and thus guiding specific therapy and avoiding unwarranted interventional procedures such as biopsy or arthroscopy.
Teaching points
• *Cystic lesions are common in knee MRI and the commonest, the Baker's cyst, has an incidence of 38 %.*
• *Synovial cysts, meniscal cysts, normal knee bursae and recesses have characteristic MR appearances.*
• *Miscellaneous "cyst-like" lesions may require a more dedicated MR protocol for a correct diagnosis.*

E. Perdikakis (✉) · V. Skiadas
Department of Radiology, 412 General Military Hospital-212 Mobile Army Surgical Hospital, Terma Lefkou Pyrgou, Xanthi 67100, Greece
e-mail: perdikakis_ev@yahoo.gr

Keywords Knee · MRI diagnosis · Cyst · Bursae · Recesses

Introduction

Given the fact that magnetic resonance imaging (MRI) is being performed more frequently for assessment of the knee joint (e.g. post-traumatic, in sport injuries, in rheumatological disorders, in oncological imaging), the number of incidental cystic and "cyst-like" lesions in and around the knee joint found on routine knee MRI scans has also increased [1–4]. The vast majority of these lesions are benign, ranging from benign cysts to complications of underlying diseases and many of them demonstrate characteristic features on MRI, thus allowing a confident diagnosis to be made [1–6]. Knowledge of the common anatomical locations and appearances of bursae, recesses, cysts and ganglia is necessary so that radiologists do not misinterpret these benign entities as soft-tissue tumours [1–8]. It is of paramount importance for the radiologist to be aware of the MRI features because understanding the spectrum of appearances of the various benign cystic lesions is vital for optimal patient management. This article is intended to be a comprehensive pictorial review of the most common and uncommon benign cystic and "cyst-like" lesions in and around the knee joint. For easier classification purposes, benign cysts were subdivided into categories as following: (1) synovial cysts, (2) ganglion cysts, (3) meniscal cysts and (4) intraosseous cysts. Similarly, "cyst-like" lesions were subclassified into the following: (1) normal knee bursae, (2) normal knee recesses and (3) miscellaneous cyst-like lesions.

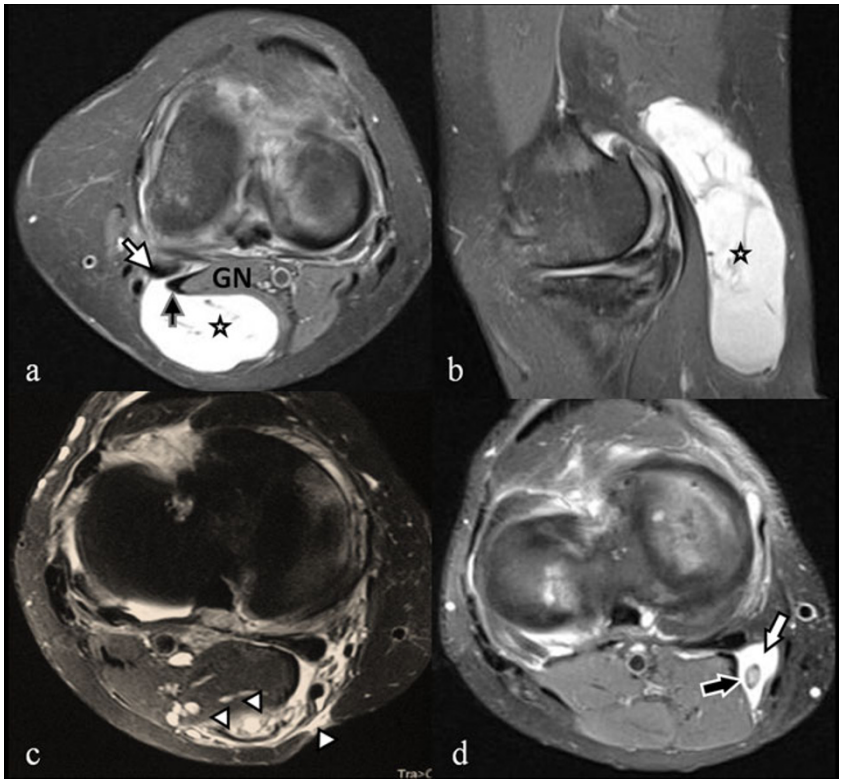

Fig. 1 *Popliteal cysts.* The axial (**a**) and sagittal (**b**) fat saturated proton density weighted images show a large multiseptated popliteal cyst (*asterisks*) emerging between the medial gastrocnemius tendon (*black arrow*) and the semimembranosus tendon (*white arrow*) and abutting the medial gastrocnemial muscle belly (*GN*). The axial (**c**) fat saturated proton density weighted image shows a ruptured popliteal cyst (*arrowheads*). The axial (**d**) fat saturated proton density weighted image demonstrates a Baker's cyst (*white arrow*) with a single loose osteocartilaginous body inside the cyst (*black arrow*)

Benign cysts

Synovial cysts

Synovial cysts are defined as juxta-articular fluid collections that are lined by synovial cells [1, 2]. The synovial lining is the characteristic histological feature that distinguishes them from other juxta-articular fluid collections [1, 2, 6, 8]. From a pathophysiological point of view a synovial cyst represents a focal extension of joint fluid that may extend in any direction and may, or may not, communicate with the joint. They can be encountered as incidental findings in MR examinations, but regarding their aetiology, they have been associated with other underlying knee disorders such as osteoarthritis, trauma, rheumatoid arthritis, gout, systemic lupus erythematosus and juvenile rheumatoid arthritis [1, 2, 4–6]. Although usually asymptomatic, they can manifest with pain and swelling. The most common examples of a synovial cyst in the knee are the popliteal cyst (Baker's cyst) and the proximal tibiofibular joint (PTFJ) synovial cyst.

The term popliteal cyst is a "misnomer" since it does not represent a true cyst, but actually corresponds to a fluid distension of the gastrocnemius-semimembranosus bursa, which occasionally communicates with the knee joint [6, 8]. Regarding its pathogenesis, a valvular mechanism between the knee joint and the bursa has been implicated, which allows joint fluid to communicate in a unidirectional mode. On MRI, they manifest as well defined unilocular or multilocular cystic masses, located posteromedially, arising between the tendon of the semimembranosus and the medial head of gastrocnemius [1, 2, 4–8]. Baker's cyst can be effectively diagnosed with MRI since the fluid-distented gastrocnemius-semimembranosus bursa is easily depicted on T2-weighted MR images, especially in the axial plane. Fluid signal intensity is seen in all sequences in cases of popliteal cysts [8, 9]. Nevertheless, complications such as haemorrhage, rupture, the presence of intra-articular loose

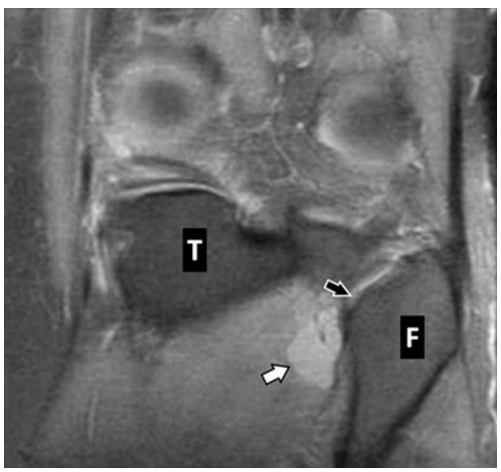

Fig. 2 *Ganglion cyst of the proximal tibiofibular joint.* The coronal fat saturated proton density weighted image shows a ganglion cyst (*white arrow*) emerging with a short neck (*black arrow*) from the proximal tibiofibular joint (*T* tibia, *F* fibula)

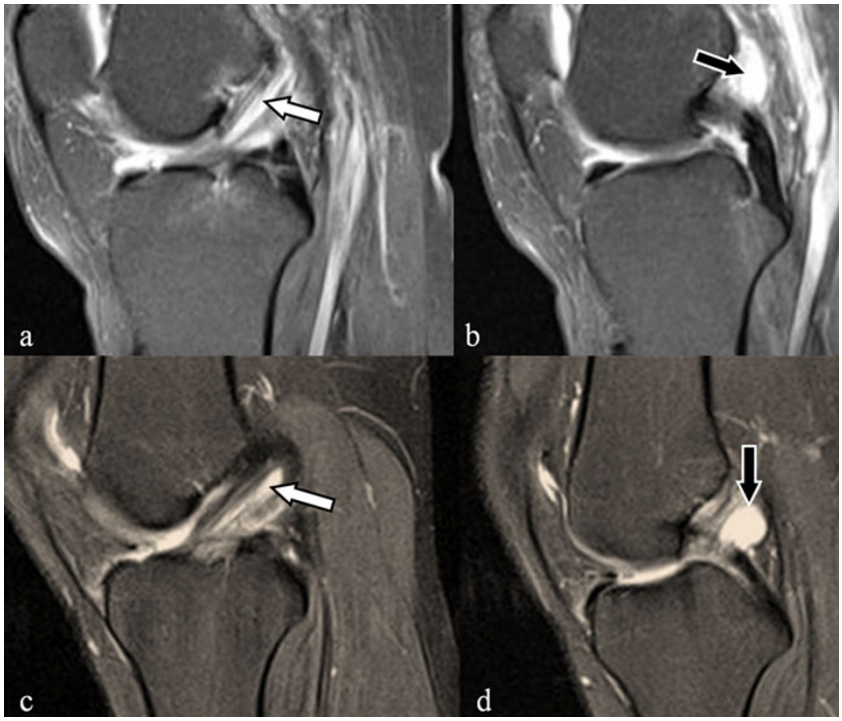

Fig. 3 *ACL ganglion cysts.* Two sequential sagittal fat saturated proton density weighted images in two different patients (*upper and lower row*) demonstrating a cystic lesion (*black arrow*) at the upper segment of the ACL with part of the lesion (*white arrow*) dispersing into the ACL fibres

bodies and synovial proliferative reaction-diseases may produce a more heterogeneous appearance. Differential diagnosis from other cyst-like lesions and soft tissue tumours is thus imperative and requires a dedicated contrast-enhanced MRI examination protocol in the aforementioned cases [8–13]. Increased signal intensity within the cyst on T1-weighted images may appear in an infected or haemorrhagic cyst. The cyst may extend to any direction, but most commonly inferomedially. Lateral or intramuscular extension is observed relatively rare. A ruptured popliteal cyst is efficiently demonstrated as a high signal intensity oedema dispersing into the adjacent soft tissues and fascial planes on fat-suppressed T2-weighted sequences (Fig. 1).

The proximal tibiofibular joint (PTFJ) synovial cyst is believed to represent a joint capsule herniation, due to increased intra-articular pressure [14–16]. On T1-weighted and T2-weighted MR sequences the lesion appears as a homogeneous often fusiform fluid collection in contact with the proximal tibiofibular joint, while a communicating neck leading from the cyst into the PTFJ is sometimes also illustrated [14–16]. Increased signal intensity on T2-weighted images of the peroneally innervated anterior compartment musculature may be present in cases of common peroneal nerve impingement. Erosion of adjacent bone may also be seen in cases of large cysts. Differential diagnosis from soft tissue and nerve sheath tumours with myxomatous or cystic degeneration may be required (Fig. 2).

Ganglion cysts

A ganglion cyst is defined as a benign cystic mass that is surrounded by dense connective tissue, without a synovial

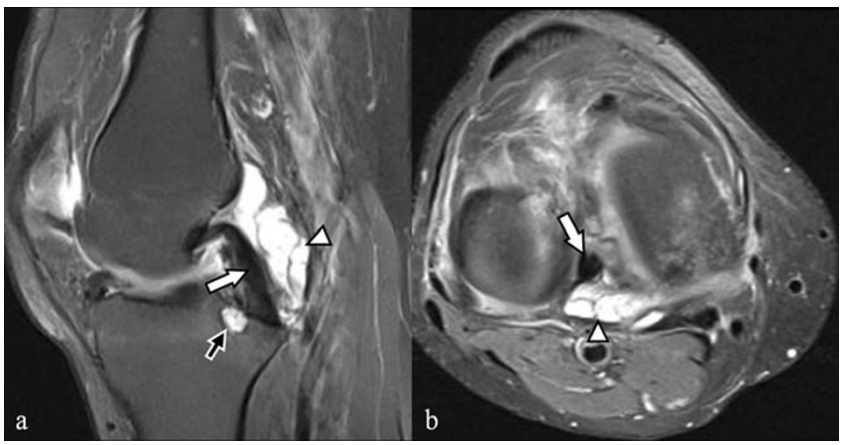

Fig. 4 *PCL ganglion cyst.* The sagittal (**a**) and axial (**b**) fat saturated proton density weighted images show a multiloculated septated cyst (*arrowheads*) located in contact with the PCL (*white arrows*) and along its dorsal surface. Note a small insertional tibial cyst (*black arrow*)

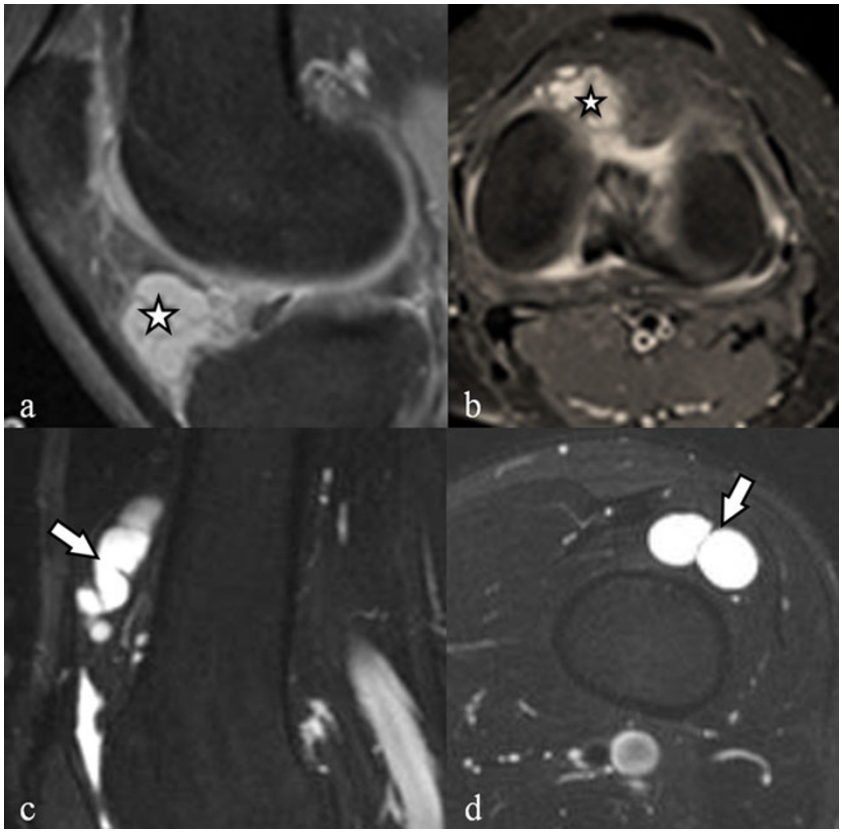

Fig. 5 *Hoffa's fat pad ganglion cysts*: the sagittal (**a**) and axial (**b**) fat saturated proton density weighted images in two different patients demonstrate a multiloculated septated cystic lesion (*asterisks*) within the Hoffa's fat pad. *Ganglion cyst of the suprapatellar bursa*: the sagittal (**a**) and axial (**b**) fat saturated T2-weighted images show a lobulated cystic lesion (*arrows*) in the suprapatellar bursa

lining and is filled with a gelatinous fluid rich in hyaluronic acid and other mucopolysaccharides. Ganglia are traditionally divided into the following categories: intra-articular, extra-articular, intraosseous and (rare) periosteal.

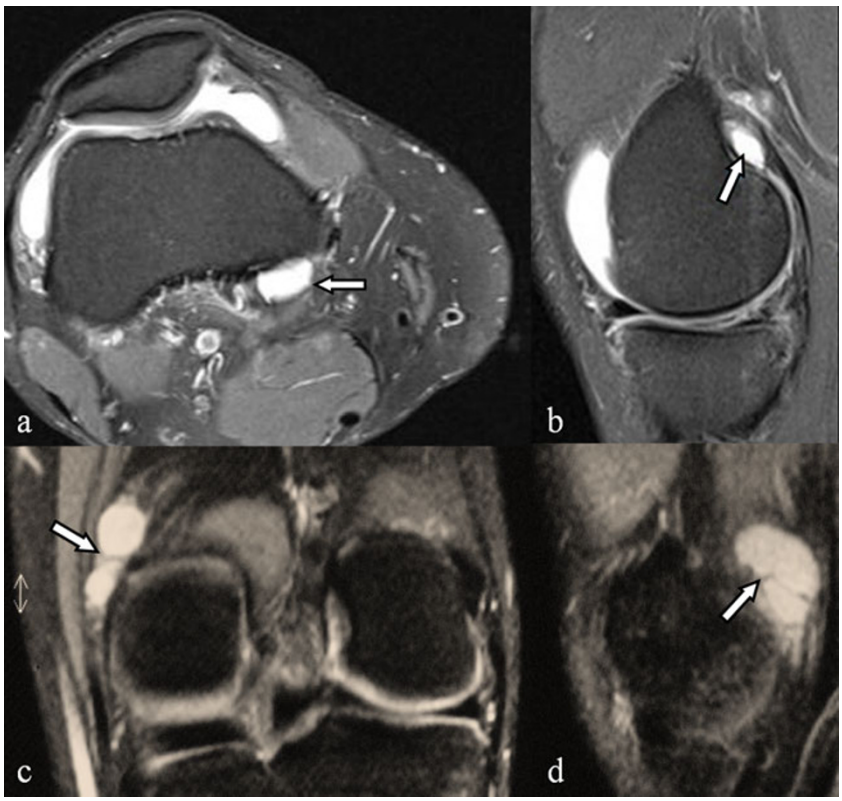

Fig. 6 *Extra-articular ganglion cysts.* The axial (**a**) and sagittal (**b**) fat saturated proton density weighted images demonstrate a unilocular cystic fluid collection consistent with an extra-articular ganglion cyst (*arrows*). The coronal (**c**) and sagittal (**d**) fat saturated proton density weighted images show a multilocular extra-articular ganglion cyst (*arrows*)

Fig. 7 *Common peroneal nerve sheath ganglion cyst.* The axial (**a**) T1-weighted, (**b**) contrast-enhanced fat saturated T1-weighted, (**c**) fat saturated proton density weighted images and two sequential coronal (**d**, **e**) fat saturated proton density weighted images show a cystic lesion (*arrows*) at the lateral aspect of the fibula head extending caudally

Intra-articular ganglia They are quite uncommon cystic lesions and typically arise from the cruciate ligaments, most commonly from the anterior cruciate ligament (ACL) [9, 11, 17, 18] In MRI part of the lesion is interspersed within the ACL fibres and it may extend anteriorly towards the Hoffa's fat pad or posteriorly towards the femoral intercondylar fossa [1, 2, 19]. Rarely it may be demonstrated between the ACL and posterior cruciate ligament (PCL). PCL ganglia have a more typical appearance and present as well-defined multilocular cysts adjacent to and along the dorsal PCL surface [1, 2, 8, 9]. Differential diagnosis should be made from a posteromedial meniscal cyst extending centrally within the joint predominantly posterior to the PCL. Ganglia within Hoffa's fat pad or in the suprapatellar recess-bursa usually appear as well-defined multilocular cysts and are most commonly encountered anterior to the anterior horn of the lateral meniscus [6, 8, 19]. An intrahoffatic lesion or a synovial lesion such as haemangioma or synovial sarcoma may be misinterpreted as a ganglion cyst within the fat pad and contrast-enhanced MRI is warranted in such cases for differential diagnosis (Figs. 3, 4 and 5).

Extra-articular ganglia Ganglion cysts may be encountered in any of the extra-articular soft tissues around the knee, including the joint capsule, tendons, ligaments, bursae, muscles and nerves. In rare cases, extra-articular ganglia may communicate with the joint cavity [1, 2, 6–8, 11–13]. On MR images they present as well-defined rounded or lobulated fluid collections, often with associated peripheral fluid-filled pseudopodia and sharply defined internal septations ("bunch of grapes appearance"). On T2-weighted images, ganglia appear with high signal intensity. On T1-weighted images, the signal intensities of ganglia range depending on their protein concentration. Associated bone erosion and pericystic oedema have been reported. The detection on MRI of a possible communication between the ganglion and the joint capsule is of great importance in preoperative planning because of the possibility of recurrence. MRI is also the imaging modality of choice for depicting muscle denervation changes in cases of nerve sheath ganglion cysts [20, 21]. These cysts are most frequently associated with the common peroneal nerve and its branches and nerve compression may result in foot drop and paraesthesia over the dorsum of the foot [20,

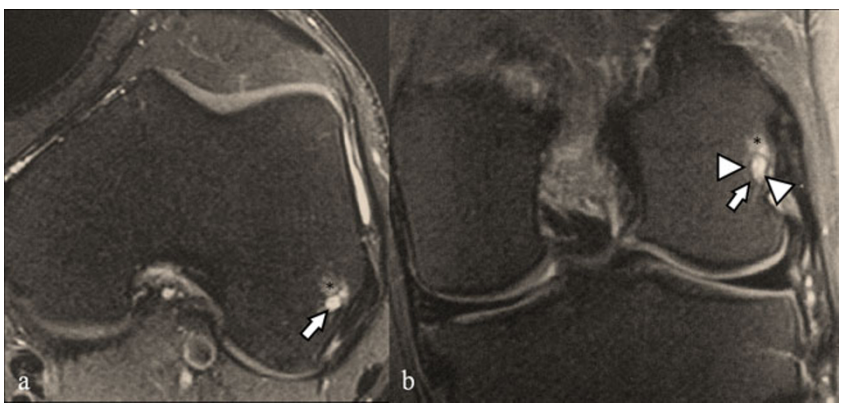

Fig. 8 *Intraosseous ganglion cyst.* The axial (**a**) and coronal (**b**) fat saturated proton density weighted images demonstrate a solitary, unilocular cystic lesion (*arrows*). Note the sclerotic rim (*arrowheads*) and mild reactive bone oedema (*asterisk*)

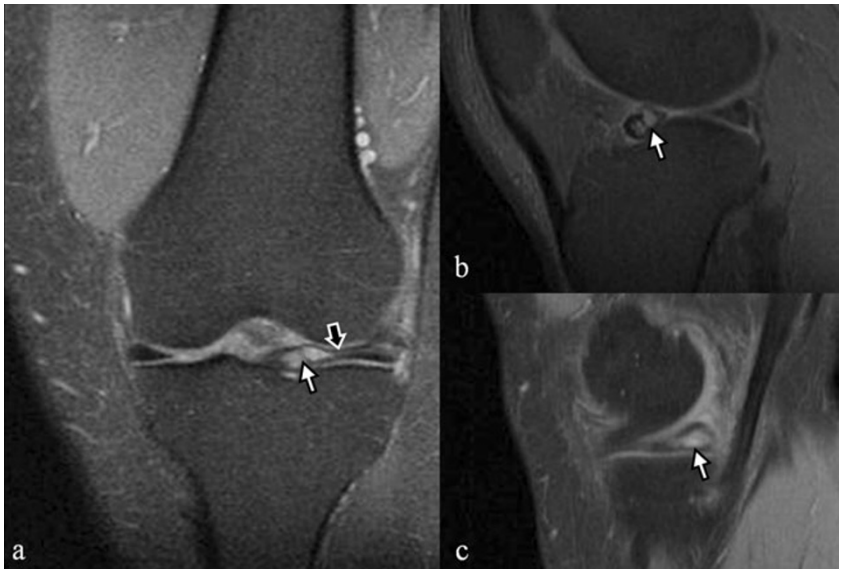

Fig. 9 *Intrameniscal cysts.* The coronal (**a**) fat saturated proton density weighted image shows a small cystic fluid collection inside the anterior horn of the lateral meniscus (*white arrow*) communicating with a horizontal meniscal tear (*black arrow*). The sagittal (**b**), (**c**) fat saturated proton density weighted images in two different patients show intrameniscal cysts of the anterior horn of the lateral meniscus (in **b**) and of the posterior horn of the medial meniscus (in **c**)

21]. MRI can contribute to treatment planning because it allows visualisation of both the cyst and the presence of oedema in the innervated muscles [20, 21]. Detection of MR signs of muscle denervation should be regarded as indicative of surgical nerve decompression. (Figs. 6 and 7).

Intraosseous ganglia These lesions are located in the epiphyseal-metaphyseal region of long bones, most commonly the tibia, often within subchondral bone, adjacent to a joint or in proximity to ligament insertion sites [7, 17, 18, 22]. Their pathogenesis is unclear and unknown and there is still debate as to whether they are distinct from degenerative, insertional or post-traumatic cysts. Regarding MRI appearance, they manifest as solitary, unilocular or multilocular, and a sclerotic rim is usually present. Differential diagnosis may be necessary from primary epiphyseal bone tumours, such as giant cell tumour, clear cell chondrosarcoma and chondroblastoma and it can also be extremely difficult to differentiate from a simple bone cyst (Fig. 8).

Periosteal ganglia They are extremely rare and are thought to be produced by mucoid degeneration and cyst formation of the periosteum [1, 2, 6–9]. They are most commonly located in the proximal tibial shaft, in proximity to pes anserinus. On MR images they typically appear as periosteally based, well-defined homogeneous lesions with fluid signal intensity. Superficial cortical erosion and scalloping, as well as reactive new bone formation may be present. Other lesions of periosteal origin, such as periosteal chondroma, subperiosteal hematoma, chronic subperiosteal abscess or malignant soft tissue tumours, mainly when they erode the adjacent bone and cause periosteal reaction, may need differential diagnosis from a periosteal ganglion.

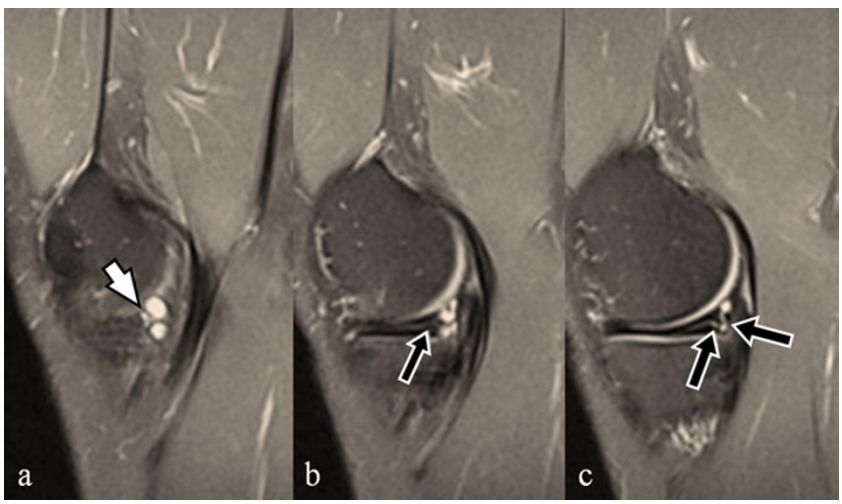

Fig. 10 *Parameniscal cyst.* Three sequential sagittal (**a**–**c**) fat saturated proton density weighted images demonstrating a lobulated cystic fluid collection (*white arrow*) in contact with the medial meniscus and arising with a short neck (*black arrows*) from a horizontal meniscal tear

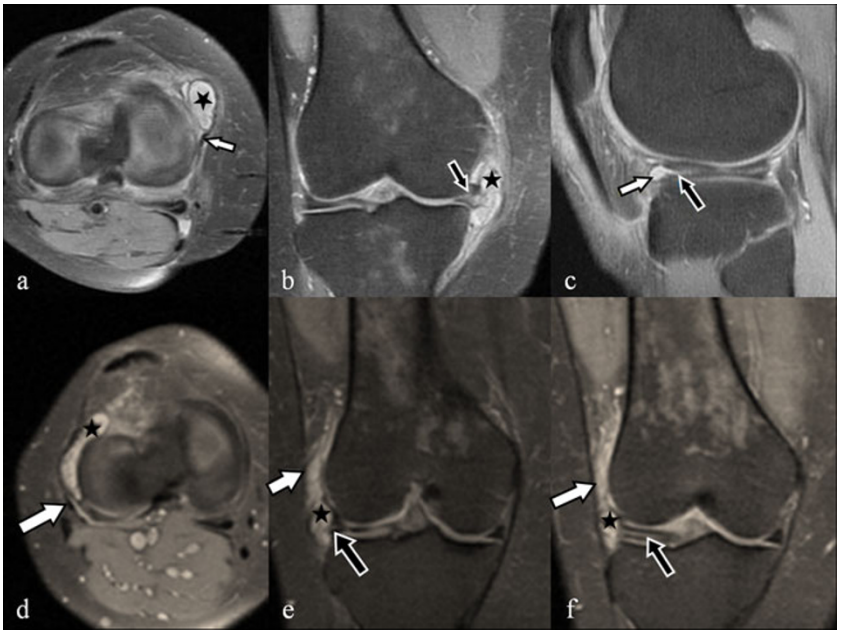

Fig. 11 *Medial parameniscal cyst*: axial (**a**) and coronal (**b**) fat saturated proton density weighted image demonstrating a parameniscal cyst (*asterisk*) anterior to the MCL (*white arrow*) arising from a complex tear of the body of medial meniscus (*black arrow*). *Anterolateral parameniscal cyst*: the sagittal (**c**) fat saturated proton density weighted image shows a parameniscal cyst (*small white arrow*) extending anteriorly within the Hoffa's fat pad and continuity with a horizontal tear of the body of the lateral meniscus is noted (*black arrow*). *Lateral parameniscal cyst*: axial (**d**) and two sequential coronal (**e** and **f**) fat saturated proton density weighted images demonstrate a parameniscal cyst (*asterisk*) deep to iliotibial tract (*thick white arrows*) communicating with a lateral meniscal horizontal tear (*black arrows*)

Meniscal cysts

Meniscal cysts are divided into *intrameniscal* and *parameniscal* cysts [23–27]. An intrameniscal cyst is a focal collection of fluid located within the meniscus. A parameniscal cyst is a focal joint fluid collection located adjacent to a meniscus. Both types of cysts are associated with a meniscal tear [23–28]. Direct communication with the meniscal tear may or may not be demonstrated on MR images. Meniscal cysts are typically demonstrated in all pulse sequences as well-defined cystic masses with fluid signal intensity [23–28]. Occasionally they may demonstrate isointensity to skeletal muscles on T1-weighted images, due to haemorrhage or high protein content. In addition, low signal intensity on T2-weighted images may be secondary to water resorption by parameniscal tissues with residual desiccated cyst contents or due to haemosiderin deposition. Most parameniscal cysts are lobulated and internally septated and may rarely cause adjacent bone erosion [23–28]. The commonest medial parameniscal cyst is that adjacent to the posterior horn of the meniscus, since tears there are far more common. The commonest location for a lateral paremeniscal cyst is adjacent to the anterior horn or the body of the lateral meniscus. Since the lateral meniscus is not tightly bound to the joint capsule, parameniscal cysts originating from the anterior horn and body of lateral meniscus may penetrate the lateral supporting structures and extend even deep to the iliotibial tract (Figs. 9, 10 and 11).

Intraosseous cysts

Intraosseous cysts can be classified into intraosseous ganglion cysts, subarticular degenerative cysts (geodes) and insertional (avulsion-traction) cysts.

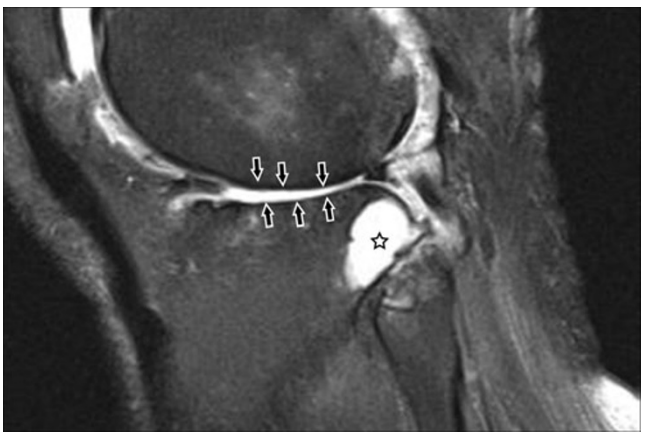

Fig. 12 *Subarticular cyst (geode).* The sagittal fat saturated proton density weighted image shows a cystic lesion (*asterisk*) in the subarticular surface of the lateral tibial condyle at the proximal tibiofibular joint. Note chondral defects of the tibial-femoral articular surfaces (*black arrows*)

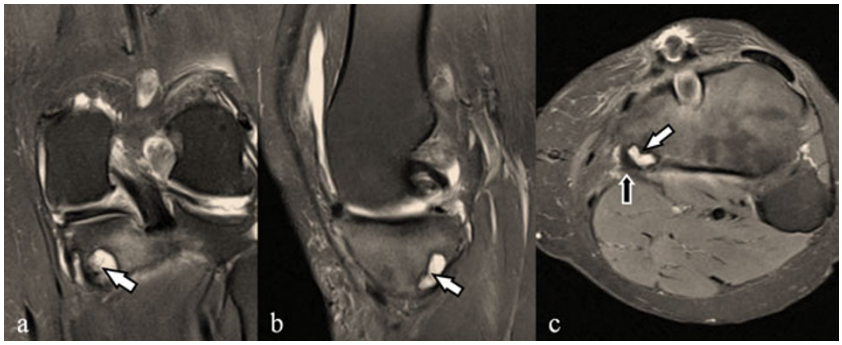

Fig. 13 *Semimembranosus insertional cyst.* The coronal (**a**), sagittal (**b**) and axial (**c**) fat saturated proton density weighted images show an intraosseous cyst (*white arrows*) located at the semimembranosus insertion. Semimembranosus tendon is shown with a *black arrow.* Findings of ACL reconstruction are also visible

Intraosseous ganglion cysts These are covered above in the "Intraosseous ganglia" section.

Degenerative or subarticular cysts (geodes) Geodes are not true cysts, since they do not have an epithelial lining [29–34]. They are usually associated with osteoarthritis and most of the times they are multiple, small cystic lesions located in both opposing sides of weight-bearing regions of the knee joint [29–34]. Common osteoarthritic changes such as osteophyte formation, absence of overlying cartilage, joint space narrowing and presence of marked surrounding bone oedema are common accompanying diagnostic clues in MR diagnosis [29–34]. These features are usually adequate to differentiate geodes from other cystic lesions that can be encountered in the same anatomic area of the bone, such as insertional and ganglion cyst, intraosseous abscess, giant cell tumour, chondroblastoma and chondrosarcoma (Fig. 12).

Insertional cysts As their name implies, they most likely originate from focal bone resorption due to chronic avulsive and traction stress at the insertional site of the ligament [1, 2, 6–9]. They are most commonly observed at the cruciate or at the meniscotibial ligamentous attachments. Regarding MRI, they are manifested as small, sharply and well defined, usually homogeneous fluid-filled lesions, surrounded by an outer low-signal margin due to fibrous tissue. Most of the times there is no perilesional bone marrow oedema, although it has been described in large insertional cysts, possibly due to bone weakening and microfractures (Fig. 13).

Cyst-like lesions

Normal knee bursae

Numerous bursae can be encountered around the knee joint and their primary action is to reduce friction between adjacent moving structures, such as tendons, ligaments and bone surfaces [6–9, 35, 36]. From a histological point of view they are synovium-lined structures and are usually collapsed but may often contain a small amount of synovial fluid. Typically are not visible on MRI, unless they are inflamed from various causes (hence the term bursitis) [6–9, 35, 36]. In the following classification, an anatomical location-based scheme (anterior-medial-lateral-posterior) is used for descriptional purposes:

Anterior bursitises

Suprapatellar bursitis The suprapatellar bursa lies between the quadriceps tendon and the femur. It commonly communicates with the knee joint cavity, unless the suprapatellar

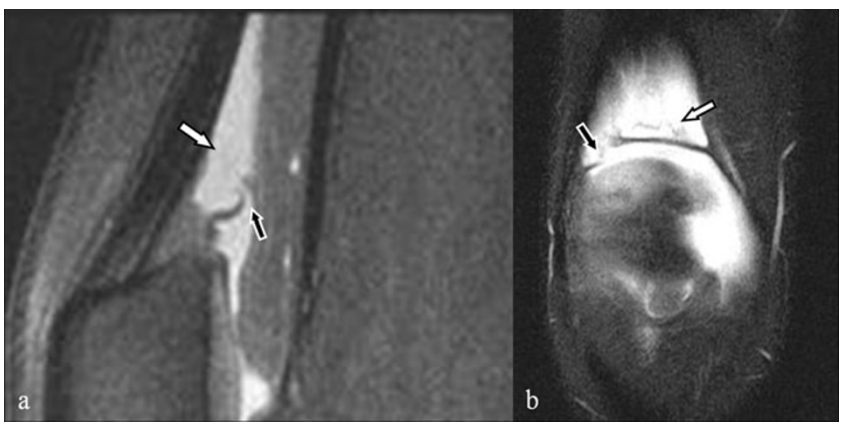

Fig. 14 *Suprapatellar bursa.* The sagittal (**a**) and coronal (**b**) fat saturated proton density weighted images shows the suprapatellar bursa (*white arrow*) with a partially perforated suprapatellar plica (*black arrow*)

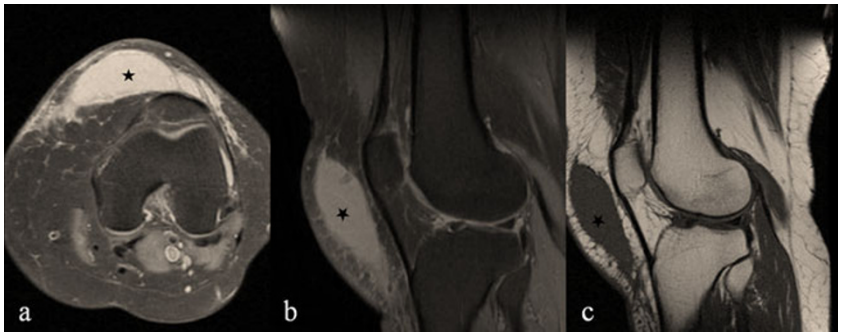

Fig. 15 *Prepatellar bursitis.* The axial (**a**), sagittal (**b**) fat saturated proton density weighted and the sagittal (**c**) T1-weighted images demonstrate a distended prepatellar bursa (*asterisk*)

plica, a normal embryonic remnant, fails to perforate and involute. In such cases, MRI reveals a focal fluid accumulation anterior to the distal part of femur, separated from the knee joint by a thin intact suprapatellar plica [1, 2, 6–9]. MR signal may be heterogeneous in chronic post-traumatic bursitis and differential diagnosis from pigmented villonodular synovitis (PVNS), haemangioma or synovial sarcoma should be made. Loose bodies and free osteochondral fragments may be present within this bursa, if it communicates with the knee joint (Fig. 14).

Prepatellar bursitis The prepatellar bursa is located anteriorly, between the patella and the subcutaneous tissues, adjacent to the proximal patellar tendon. Prepatellar bursitis is an inflammation of the prepatellar bursa either due to acute trauma (direct fall on to the knee) or to chronic repetitive microtrauma (housemaid's knee, carpet-layer's knee) [6, 8–10]. On MRI prepatellar bursitis presents as a focal fluid collection in all pulse sequences anterior to the patella and the superior part of the patellar tendon. However, inflammatory or haemorrhagic bursitis may present as a more complex, poorly defined, septated collection with heterogeneous signal intensity and internal debris (Fig. 15).

Superficial infrapatellar bursitis The superficial infrapatellar or pretibial bursa is located between the tibial tubercle and the overlying skin. It is an uncommon site for bursitis, but direct trauma or occupational overuse (clergyman's knee) may result in inflammation and micro-haemorrhage) [1, 2, 6]. The characteristic MRI finding is a focally poorly defined fluid collection anterior to the tibial tubercle.

Deep infrapatellar bursitis The deep infrapatellar bursa is located between the posterior margin of the distal part of the patellar tendon and the anterior tibia, beneath Hoffa's fat pad [1, 2, 6, 8, 35]. There is no communication with the knee joint and is usually inflamed in overuse sports injuries, most commonly in runners and jumpers. On MRI a fluid collection is seen between the distal patellar tendon and the tibia. However, a small amount of fluid in the deep infrapatellar bursa may be present in asymptomatic individuals, and for that reason clinical correlation is warranted (Fig. 16).

Medial bursitises

Anserine bursitis (Pes anserinus bursitis) The anserine bursa lies deep to the pes anserinus, superficial to the tibial insertion of the medial collateral ligament and the medial tibial condyle, and slightly distal to the insertion of the semimembranosus tendon [35–37]. Clinically, anserine bursitis may mimic a medial meniscus tear or injury of the MCL and is more commonly seen as a sports injury in runners [1, 2, 6–9, 35]. Its MR appearance is a homogeneous, ovoid fluid collection in the aforementioned location. The differential diagnosis includes an atypical synovial cyst and a parameniscal cyst, lesions that may also be found in

Fig. 16 *Deep infrapatellar bursitis.* The sagittal fat saturated proton density weighted image demonstrates a small fluid collection in the deep infrapatellar bursa (*arrow*), between the distal patellar tendon and the tibia

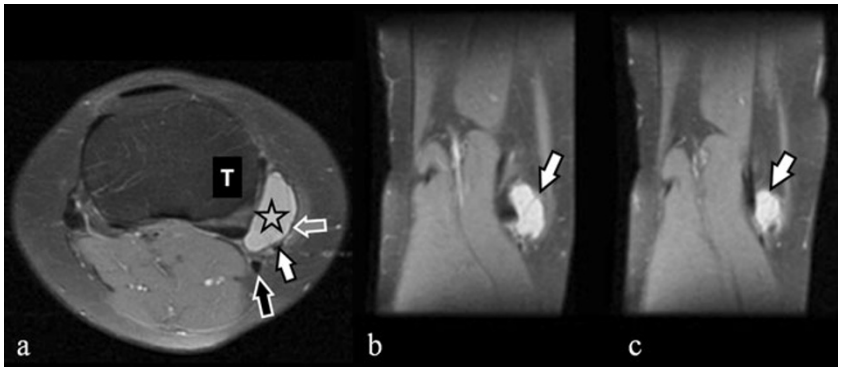

Fig. 17 *Pes anserinus bursitis.* The axial (**a**) and coronal (**b**, **c**) fat saturated proton density weighted images show a cystic fluid collection (noted with *asterisk* in **a** and *arrows* in **b**, **c**) located between the medial aspect of the tibia and the pes anserinus tendons: sartorius muscle (*grey arrow*), gracilis tendon (*white arrow*) and semitendinosus tendon (*black arrow*). *T* tibia

this position. Chronic pes anserinus bursitis is reported more frequently and found in overweight middle-aged to elderly women and in patients with underlying degenerative joint disease or rheumatoid arthritis. Its MRI appearance is less specific. Thickened synovial lining and heterogeneous signal fluid intensity have been reported. The differential diagnosis of chronic pes anserinus bursitis includes PVNS and synovial haemangioma (Fig. 17).

Medial collateral ligament bursitis (MCL bursitis) The medial collateral ligament bursa lies vertically between the superficial and deep layer of MCL [38–42]. MCL bursitis as an isolated finding is extremely rare, with most cases associated with arthritides and medial intra-articular pathology. MCL bursitis on MR images is demonstrated as a vertically elongated, well-defined fluid collection between the superficial and deep layer of the MCL [38–42]. Separate femoral and tibial components may be observed, and this has also been proved in cadaveric studies. Meniscal cyst and ganglion cyst should also be considered in the differential diagnosis of MCL bursitis (Fig. 18).

Semimembranosus-tibial collateral ligament bursitis The semimembranosus-tibial collateral ligament (SMTCL) bursa is located between the semimembranosus tendon and the MCL, having a deeper portion extending between the semimembranosus tendon and medial tibial condyle [6, 8]. On MRI, SMTCL bursitis is demonstrated as a longitudinal fluid collection along the semimembranosus tendon, in a pattern surrounding the tendon [6, 8]. On axial images the SMTCL bursitis has the shape of an inverted U and on coronal images it has a semilunar configuration [6, 8]. The deep part is located proximally between the semimembranosus tendon and the medial tibial condyle, adjacent to the posterior horn of the medial meniscus, though the superficial part lies distally between the semimembranosus tendon and the MCL. These two parts are joined along the anterosuperior aspect of the semimembranosus tendon [6, 8]. Differential diagnosis of SMTCL bursitis should be done from a parameniscal cyst, since its proximal end abuts the posterior horn of the medial meniscus (Fig. 19).

Lateral bursitises

Iliotibial bursitis The iliotibial bursa is located between the distal part of the iliotibial band, near its insertion on Gerdy's tubercle, and the adjacent tibial surface. It may mimic iliotibial tendinitis and lateral meniscal or lateral collateral ligamentous pathology [1, 2, 6, 8]. On MR images iliotibial bursitis is demonstrated as a well-defined fluid collection between the insertion of the distal iliotibial band and the adjacent bony surface.

Lateral/fibular collateral ligament-biceps femoris bursitis (LCL bursitis) The fibular collateral ligament (FCL)-biceps

Fig. 18 *MCL bursitis.* The coronal fat saturated proton density weighted image demonstrates a small fluid collection between the deep MCL (meniscofemoral ligament: *grey arrow*, meniscotibial ligament: *black arrow*) and the superficial portion (*white arrow*) of the MCL

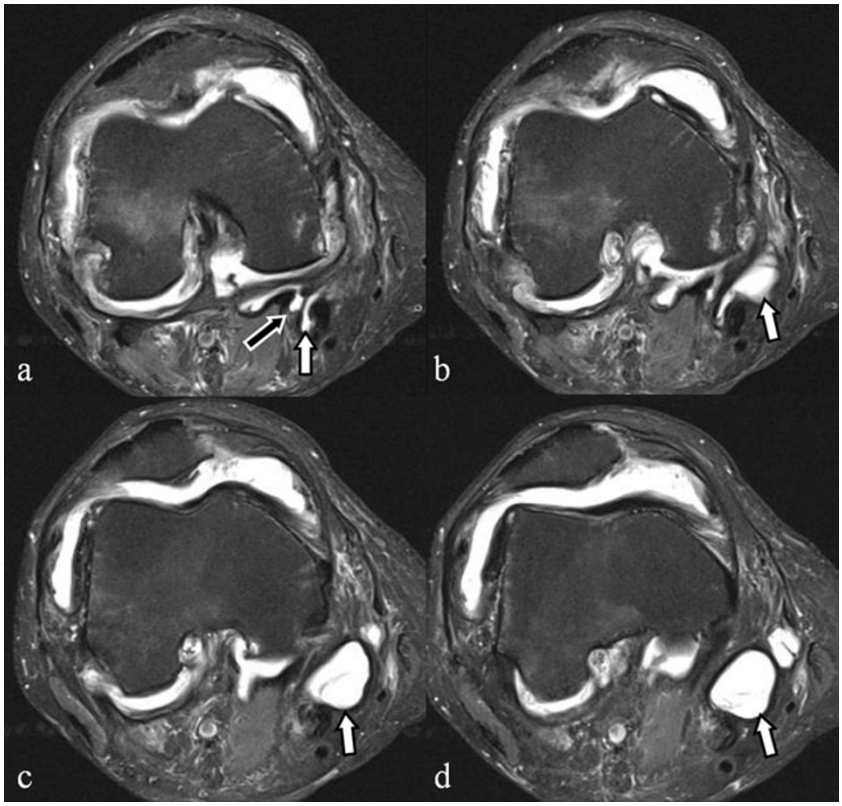

Fig. 19 *Semimembranosus-medial collateral ligament bursitis.* The axial (**a**–**d**) fat saturated proton density weighted images show a fluid distended semimembranosus–MCL bursa (*white arrow*). In contact with the semimembranosus-MCL bursa a small Baker cyst is demonstrated (*black arrow*). In image (**b**) the lesion takes the typical configuration of a distended semimembranosus-MCL bursa, that of an inverted U

femoris bursa is located superficial to the distal FCL and deep to the anterior arm of the long head of the biceps femoris muscle [1, 2, 6, 8]. On axial MR images it is demonstrated as a fluid collection around the FCL, forming an inverted J-shape, whose long arm extends along the lateral aspect of the FCL and the hook is curved around the anterior edge of the FCL. The proximal portion is at the superior edge of the anterior arm of the long head of the biceps femoris muscle and the distal one is at the insertion of the FCL on the fibula head (Fig. 20).

Posterior bursitises

Gastrocnemius-semimembranosus bursitis (Posterior bursitis) The posteriorly located gastrocnemius-semimembranosus bursa (popliteal or Baker's cyst) together with its symptomatology is covered above in the synovial cyst section.

In summary, the MR characteristics of the various bursae that can be encountered around the knee joint have been

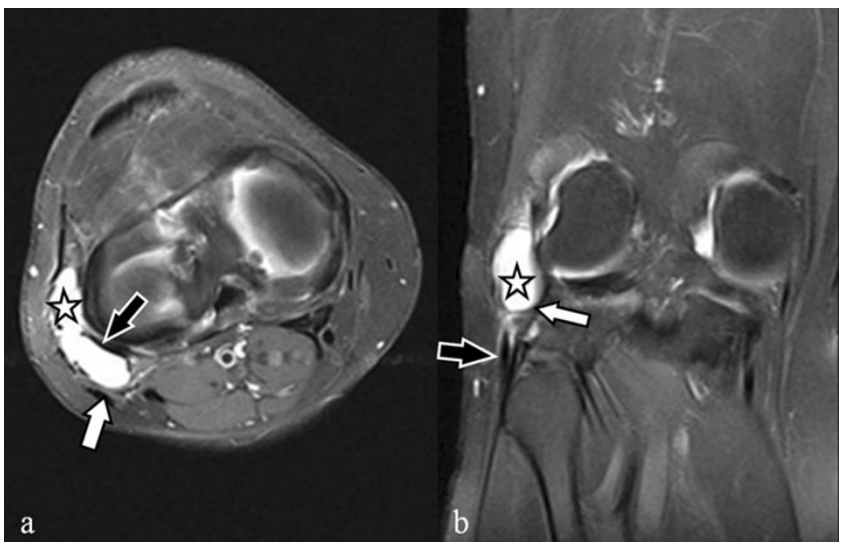

Fig. 20 *LCL bursitis.* The axial (**a**) and coronal (**b**) fat saturated proton density weighted images show a fluid collection in the dilated LCL bursa (*asterisk*). The *white arrow* points to LCL and the *black arrow* points to biceps femoris tendon

Fig. 21 *Knee recesses.* The sagittal (**a**) fat saturated proton density weighted image shows fluid in the subpopliteal-subgastrocnemius (*white arrow*) and posterior femoral recess (*black arrow*). Findings of ACL reconstruction are also visible (in *dotted line*). The axial (**b**) fat saturated proton density weighted image shows a fluid distended posterior capsular recess which is located posteriorly to the PCL. The axial (**c**) fat saturated proton density weighted image shows fluid in the subpopliteal recess (*white arrow*). A Baker cyst (with *asterisk*) and geodes (*black arrows*) at both tibial condyles are also shown. The axial (**d**) fat saturated proton density weighted image shows the central recesses (*white arrows*) with fluid extending medially and laterally deep to the patellar retinacula

presented in this section. Above and beyond correct diagnosis the radiologist can also be implicated in the clinical management of these conditions. Treatment with ultrasound-guided aspiration and local injection of long-acting analgesic and steroid may relieve symptoms and represent the optimal therapy in cases of bursitis [43–46]. Percutaneous-guided treatments have been used successfully for pain management in bursitis and have been proven effective, thus obviating the need for surgical therapy [43–46].

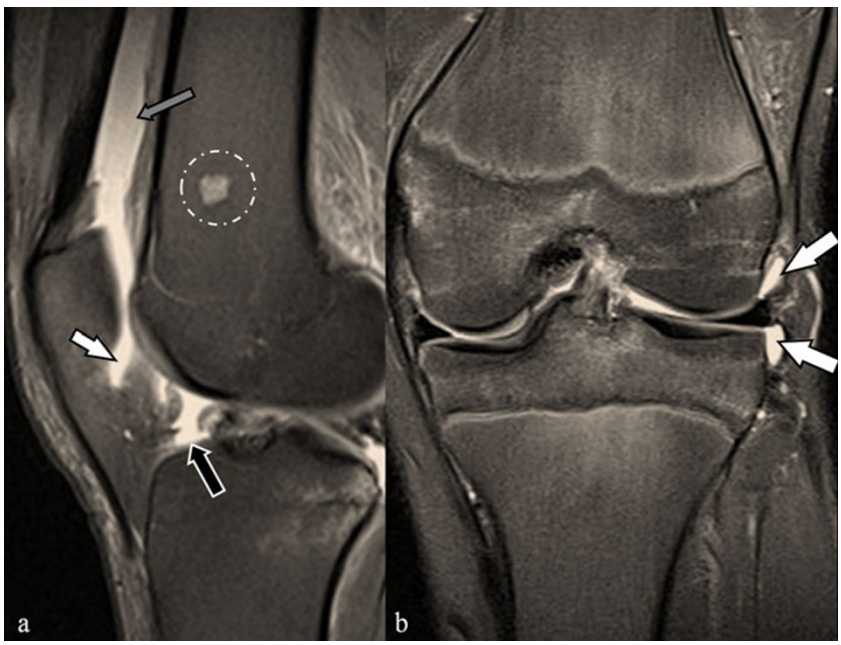

Fig. 22 *Knee recesses.* The sagittal (**a**) fat saturated proton density weighted image shows fluid in the suprahoffatic recess (*white arrow*), in the infrahoffatic recess (*black arrow*) and in the suprapatellar pouch (*grey arrow*). A small fluid intensity lesion in the distal femoral metaphysis (in *dotted line*) represents a small enchondroma. The coronal (**b**) fat saturated proton density weighted image shows the parameniscal recesses (*white arrows*) with fluid above and below the lateral meniscal margins at the level of the body

Fig. 23 *Popliteal artery aneurysm*: the axial (**a**) T1-weighted and the sagittal (**b**) T2-weighted GRE images show a popliteal aneurysm with thrombus and rim-like calcifications. The blood flow creates an artefact (*grey arrows*) that helps in the diagnosis. *Popliteal vein's varices*: the axial (**c**) and coronal (**d**, **e**) fat saturated proton density weighted images demonstrate lobulated cystic lesions (*black arrows*) in continuity with the popliteal vein consistent with popliteal vein varices. *White small arrow* in (**c**) points to the dilated great saphenous vein

Normal knee recesses

There are numerous anatomical knee recesses that can be demonstrated in cases of knee effusion and may be misinterpreted as cyst-like lesions [47–50]. Good knowledge of those spaces is essential in order to avoid pitfalls in MRI.

The *posterior femoral recesses (subgastrocnemius recesses)* are found posteriorly to both femoral condyles and the deep surface of the lateral and medial heads of gastrocnemius.

The *posterior capsular recesses (in the midline)* behind the PCL, may be identified as an extension of the medial femorotibial compartment.

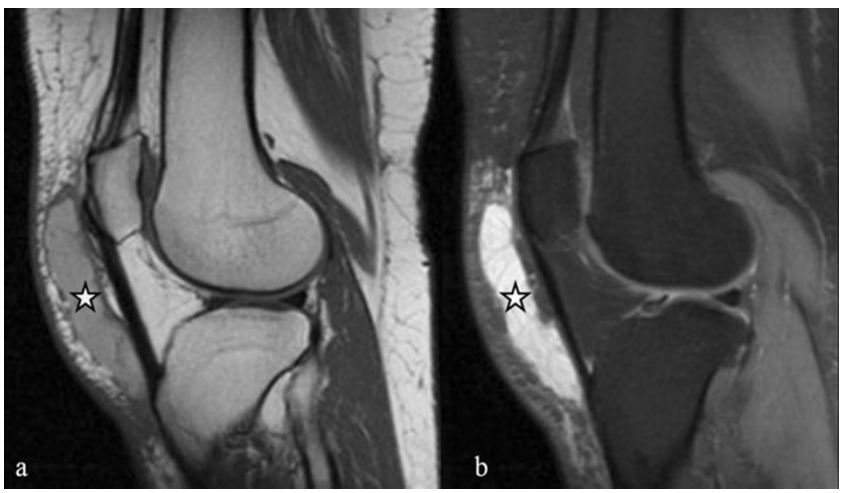

Fig. 24 *Haematoma.* The sagittal (**a**) T1-weighted and the sagittal (**b**) fat saturated proton density weighted images show a fluid collection in front of the patellar tendon with high signal intensity in T1-weighted image consistent with a haematoma

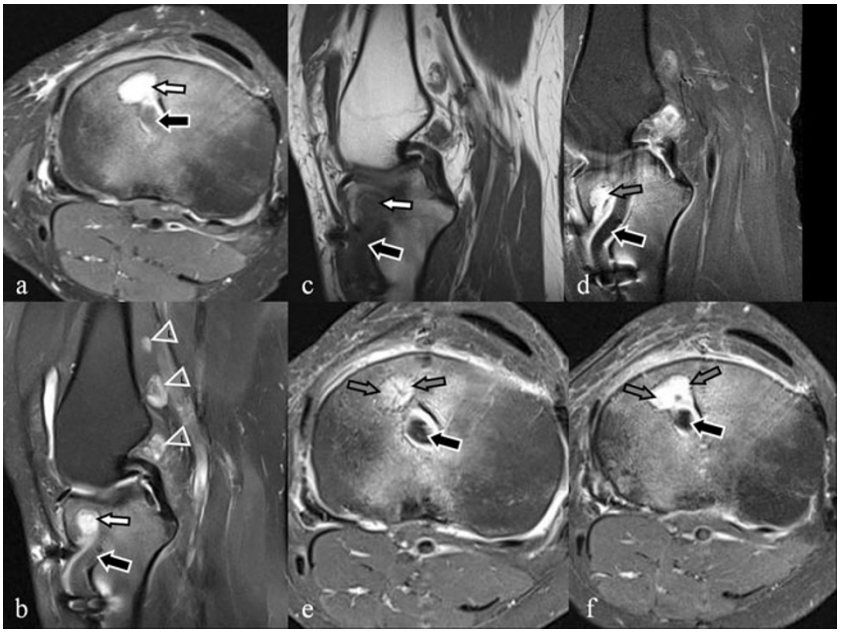

Fig. 25 *Brodie's abscess and lymph nodes in a patient with ACL reconstruction.* (**a**) Axial and (**b**) sagittal fat saturated proton density weighted, (**c**) sagittal T1-weighted, (**d**) sagittal fat saturated contrast-enhanced T1-weighted and (**e**, **f**) sequential axial fat saturated contrast-enhanced T1-weighted images. A small cystic lesion (*white arrow*) at the anterior aspect of the tibia in contact with the ACL graft (*black arrow*) with marked peripheral enhancement (*grey arrows*) and a central non-enhancing portion is depicted. The abscess was draining via a sinus tract along the ACL graft to the anterior surface of the tibia. Three small cystic-like lesions (*grey arrowheads*) in the popliteal fossa, represent enlarged lymph nodes

The *subpopliteal recess* is demonstrated between the popliteus tendon and the posterior horn of the lateral meniscus.

The *suprahoffatic recess* is at the superior part of the Hoffa's fat pad, close to the inferior border of the patella.

Fig. 26 *Synovial sarcoma.* The sagittal (**a**) and axial (**b**) fat saturated proton density weighted images show a multilocular "cyst-like" lesion near the knee joint (*white arrows*). The axial (**c**) T1-weighted and the axial (**d**) fat saturated contrast-enhanced T1-weighted images aided in the differential diagnosis by showing the solid nature of the tumour. The lesion demonstrated intense contrast enhancement except for a peripherally located necrotic part (*grey arrows*)

The *infrahoffatic recess* lies anterior to the inferior portion of the infrapatellar plica (also called ligamentum mucosum).

The *anterior tibial recess*, is a normal capsular recess immediately anterior to the proximal tibia.

The *central synovial recess* lies between the patella/patellar ligaments and the anterior aspect of the femur.

The *parameniscal recess* lies just superior and inferior to the level of the lateral meniscus in contact with the lateral femoral and tibial condyle (Figs. 21 and 22).

Other miscellaneous cyst-like lesions

A variety of "cystic" lesions can be encountered in and around the knee joint that may complicate the differential diagnosis even more [1, 2, 6–11]. The most common benign non-tumoral are the following:

Popliteal artery aneurysms present on MR images with variable signal intensity depending on flow characteristics and pulse sequences [51, 52]. They are typically situated within the popliteal fossa. A laminated MR appearance consistent with multilayered thrombus and occasionally rim-like calcification may also be demonstrated. The lesion shows continuity with the popliteal artery, which is a hallmark in diagnosis. *Popliteal vein varices* are focal dilatations of the popliteal vein [1, 2, 6–11]. They present on MR images as lobulated masses in continuity with the popliteal vein. *Lymph nodes* located in and around the popliteal fossa may also manifest as cyst-like structures [1, 2, 6–11]. Knowledge of their location as well as of the normal MR appearance of the lymph node fatty hillum aids in the differential diagnosis. *Haematomas* may simulate a cyst but can be differentiated by its signal intensity which depends on blood products' age (haemoglobin degradation products) [53–55]. *Abscesses* that can also mimic cysts are associated with infection and inflammation in the surrounding soft tissues and occasionally underlying osteomyelitis [55–57]. Contrast enhancement is necessary for the correct diagnosis and for unmasking a possible sinus tract (Figs. 23, 24 and 25).

In addition, administration of intravenous contrast is primarily helpful in the evaluation of soft tissue masses and particularly in differentiating cysts from *malignant pseudocystic conditions* [9–13]. Solid tumours with central necrosis, cystic degeneration or myxoid stroma such as synovial sarcoma, dedifferentiated sarcoma, myxoid liposarcoma, metastases and the benign synovial haemangioma may have homogeneously high signal on T2-weighted images mimicking a cyst, but they enhance after contrast administration contrary to the cysts (Fig. 26).

Conclusion

Benign cystic and "cyst-like" lesions are a common finding inside and around the knee joint. MRI is an excellent method for demonstrating and differentiating these lesions. A radiologist should be able to identify typical MRI patterns that contribute in establishing the correct diagnosis and thus guiding specific therapy and avoiding unwarranted interventional procedures such as biopsy or arthroscopy.

Conflict of interest None.

References

1. Beaman FD, Peterson JJ (2007) MR imaging of cysts, ganglia, and bursae about the knee. Radiol Clin North Am 45:969–982
2. Beaman FD, Peterson JJ (2007) MR imaging of cysts, ganglia, and bursae about the knee. Magn Reson Imaging Clin N Am 15:39–52
3. Ghazikhanian V, Beltran J, Nikac V, Feldman M, Bencardino JT (2012) Tibial tunnel and pretibial cysts following ACL graft reconstruction: MR imaging diagnosis. Skeletal Radiol 41:1375–1379
4. Guermazi A, Hayashi D, Roemer FW et al (2010) Cyst-like lesions of the knee joint and their relation to incident knee pain and development of radiographic osteoarthritis: the MOST study. Osteoarthr Cartil 18:1386–1392
5. Janzen DL, Peterfy CG, Forbes JR, Tirman PF, Genant HK (1994) Cystic lesions around the knee joint: MR imaging findings. AJR Am J Roentgenol 163:155–161
6. McCarthy CL, McNally EG (2004) The MRI appearance of cystic lesions around the knee. Skeletal Radiol 33:187–209
7. Williams HJ, Davies AM, Allen G, Evans N, Mangham DC (2004) Imaging features of intraosseous ganglia: a report of 45 cases. Eur Radiol 14:1761–1769
8. Marra MD, Crema MD, Chung M et al (2008) MRI features of cystic lesions around the knee. Knee 15:423–438
9. Stacy GS, Kapur A (2011) Mimics of bone and soft tissue neoplasms. Radiol Clin North Am 49:1261–1286
10. Stein-Wexler R (2009) MR imaging of soft tissue masses in children. Magn Reson Imaging Clin N Am 17:489–507
11. Subhas N, Bui KL, Sundaram M, Ilaslan H, Recht MP (2009) Incidental tumor and tumor-like lesions around the knee. Semin Musculoskelet Radiol 13:353–370
12. Chung CB, Boucher R, Resnick D (2009) MR imaging of synovial disorders of the knee. Semin Musculoskelet Radiol 13:303–325
13. Papp DF, Khanna AJ, McCarthy EF, Carrino JA, Farber AJ, Frassica FJ (2007) Magnetic resonance imaging of soft-tissue tumors: determinate and indeterminate lesions. J Bone Joint Surg Am 89(Suppl 3):103–115
14. Jerome D, McKendry R (2000) Synovial cyst of the proximal tibiofibular joint. J Rheumatol 27:1096–1098
15. Mortazavi SM, Farzan M, Asadollahi S (2006) Proximal tibiofibular joint synovial cyst–one pathology with three different presentations. Knee Surg Sports Traumatol Arthrosc 14:875–879
16. Pećina HI, Borić I, Pećina TC, Smoljanović T, Pećina M (2008) Double synovial cyst of the proximal tibiofibular joint confirmed

by MRI as a cause of the peroneal tunnel syndrome. Acta Chir Orthop Traumatol Cech 75:301–305
17. Battaglia TC, Freilich AM, Diduch DR (2007) An intra-articular knee cyst in a 2-year-old associated with an aberrant anterior cruciate ligament. Knee Surg Sports Traumatol Arthrosc 15:36–38
18. Krudwig WK, Schulte KK, Heinemann C (2004) Intra-articular ganglion cysts of the knee joint: a report of 85 cases and review of the literature. Knee Surg Sports Traumatol Arthrosc 12:123–129
19. Ozkur A, Adaletli I, Sirikci A, Kervancioglu R, Bayram M (2005) Hoffa's recess in the infrapatellar fat pad of the knee on MR imaging. Surg Radiol Anat 27:61–63
20. Yazid Bajuri M, Tan BC, Das S, Hassan S, Subanesh S (2011) Compression neuropathy of the common peroneal nerve secondary to a ganglion cyst. Clin Ter 162:549–552
21. Rawal A, Ratnam KR, Yin Q, Sinopidis C, Frostick SP (2004) Compression neuropathy of common peroneal nerve caused by an extraneural ganglion: a report of two cases. Microsurgery 24:63–66
22. Başbozkurt M, Hapa O, Demiralp B (2011) Distal femoral intraosseous ganglia: cause or result of a degenerative process: 17-year follow-up of a case. Musculoskelet Surg 95:147–150
23. Anderson JJ, Connor GF, Helms CA (2010) New observations on meniscal cysts. Skeletal Radiol 39:1187–1191
24. De Smet AA, Graf BK, del Rio AM (2011) Association of parameniscal cysts with underlying meniscal tears as identified on MRI and arthroscopy. AJR Am J Roentgenol 196:W180–W186
25. McKnight A, Southgate J, Price A, Ostlere S (2010) Meniscal tears with displaced fragments: common patterns on magnetic resonance imaging. Skeletal Radiol 39:279–283
26. Quatman CE, Hettrich CM, Schmitt LC, Spindler KP (2011) The clinical utility and diagnostic performance of magnetic resonance imaging for identification of early and advanced knee osteoarthritis: a systematic review. Am J Sports Med 39:1557–1568
27. Vande Berg BC, Malghem J, Poilvache P, Maldague B, Lecouvet FE (2005) Meniscal tears with fragments displaced in notch and recesses of knee: MR imaging with arthroscopic comparison. Radiology 234:842–850
28. Wyss JF, Foye PM, Stitik TP (2010) An infected, extruded lateral meniscal cyst as a cause of knee symptoms. Am J Phys Med Rehabil 89:175–176
29. Carrino JA, Blum J, Parellada JA, Schweitzer ME, Morrison WB (2006) MRI of bone marrow edema-like signal in the pathogenesis of subchondral cysts. Osteoarthr Cartil 14:1081–1085
30. Choi JA, Gold GE (2011) MR imaging of articular cartilage physiology. Magn Reson Imaging Clin N Am 19:249–282
31. Guermazi A, Zaim S, Taouli B, Miaux Y, Peterfy CG, Genant HG (2003) MR findings in knee osteoarthritis. Eur Radiol 13:1370–1386
32. Peterfy CG, Guermazi A, Zaim S et al (2004) Whole-Organ Magnetic Resonance Imaging Score (WORMS) of the knee in osteoarthritis. Osteoarthr Cartil 12:177–190
33. Huétink K, Nelissen RG, Watt I, van Erkel AR, Bloem JL (2010) Localized development of knee osteoarthritis can be predicted from MR imaging findings a decade earlier. Radiology 256:536–546
34. Hayashi D, Xu L, Roemer FW et al (2012) Detection of osteophytes and subchondral cysts in the knee with use of tomosynthesis. Radiology 263:206–215
35. Chatra PS (2012) Bursae around the knee joints. Indian J Radiol Imaging 22:27–30
36. Nouri H, Ben Hmida F, Ouertatani M et al (2010) Tumour-like lesions of the infrapatellar fat pad. Knee Surg Sports Traumatol Arthrosc 18:1391–1394
37. Maheshwari AV, Muro-Cacho CA, Pitcher JD Jr (2007) Pigmented villonodular bursitis/diffuse giant cell tumor of the pes anserine bursa: a report of two cases and review of literature. Knee 14:402–407
38. De Maeseneer M, Shahabpour M, Pouders C (2010) MRI spectrum of medial collateral ligament injuries and pitfalls in diagnosis. JBR-BTR 93:97–103
39. De Maeseneer M, Shahabpour M, Vanderdood K, Van Roy F, Osteaux M (2002) Medial meniscocapsular separation: MR imaging criteria and diagnostic pitfalls. Eur J Radiol 41:242–252
40. Kramer J, White LM, Recht MP (2009) MR imaging of the extensor mechanism. Semin Musculoskelet Radiol 13:384–401
41. Nandi S, Parker R (2012) Deep medial collateral ligament tear during knee arthroscopy. J Knee Surg 25:79–81
42. Schein A, Matcuk G, Patel D et al (2012) Structure and function, injury, pathology, and treatment of the medial collateral ligament of the knee. Emerg Radiol 19:489–498
43. Miller JC, Palmer WE, Goroll AH, Thrall JH, Uppot RN (2009) Anesthetic and steroid injections for musculoskeletal pain. J Am Coll Radiol 6:806–808
44. Di Sante L, Paoloni M, Ioppolo F, Dimaggio M, Di Renzo S, Santilli V (2010) Ultrasound-guided aspiration and corticosteroid injection of Baker's cysts in knee osteoarthritis: a prospective observational study. Am J Phys Med Rehabil 89:970–975
45. Jose J, Schallert E, Lesniak B (2011) Sonographically guided therapeutic injection for primary medial (tibial) collateral bursitis. J Ultrasound Med 30:257–261
46. del Cura JL (2008) Ultrasound-guided therapeutic procedures in the musculoskeletal system. Curr Probl Diagn Radiol 37:203–218
47. Aydingöz U, Oguz B, Aydingöz O et al (2005) Recesses along the posterior margin of the infrapatellar (Hoffa's) fat pad: prevalence and morphology on routine MR imaging of the knee. Eur Radiol 15:988–994
48. Fenn S, Datir A, Saifuddin A (2009) Synovial recesses of the knee: MR imaging review of anatomical and pathological features. Skeletal Radiol 38:317–328
49. García-Valtuille R, Abascal F, Cerezal L et al (2002) Anatomy and MR imaging appearances of synovial plicae of the knee. Radiographics 22:775–784
50. Maurel B, Le Corroller T, Cohen M et al (2010) Infrapatellar fat pad: anterior crossroads of the knee. J Radiol 91:841–855
51. Holden A, Merrilees S, Mitchell N, Hill A (2008) Magnetic resonance imaging of popliteal artery pathologies. Eur J Radiol 67:159–168
52. Wright LB, Matchett WJ, Cruz CP et al (2004) Popliteal artery disease: diagnosis and treatment. Radiographics 24:467–479
53. Bush CH (2000) The magnetic resonance imaging of musculoskeletal hemorrhage. Skeletal Radiol 29:1–9
54. Oka K, Yakushiji T, Sato H et al (2008) Ability of diffusion-weighted imaging for the differential diagnosis between chronic expanding hematomas and malignant soft tissue tumors. J Magn Reson Imaging 28:1195–1200
55. Recht MP, Kramer J (2002) MR imaging of the postoperative knee: a pictorial essay. Radiographics 22:765–774
56. Martí-Bonmatí L, Aparisi F, Poyatos C, Vilar J (1993) Brodie abscess: MR imaging appearance in 10 patients. J Magn Reson Imaging 3:543–546
57. Soldatos T, Durand DJ, Subhawong TK, Carrino JA, Chhabra A (2012) Magnetic resonance imaging of musculoskeletal infections: systematic diagnostic assessment and key points. Acad Radiol 19:1434–1443